J Electroceram (2009) 22:357–362
DOI 10.1007/s10832-007-9180-9

Structure and ferroelectric property of Nb-doped $SrBi_4Ti_4O_{15}$ ceramics

Hua Hao · Hanxing Liu · Shixi Ouyang

Received: 19 December 2005 / Accepted: 2 June 2007 / Published online: 6 July 2007

Abstract Nb-doped $SrBi_4Ti_4O_{15}$ (SBT) was produced by conventional method. Structural and ferroelectric properties of SBT were examined as a function of niobium composition. Analyzing the structure futures of SBT by XRD, XPS and Raman spectrum, Nb^{5+} substituted Ti^{4+} to form NbO_6 octahedron and did not change the structure of SBT. The XRD patterns indicated the formation of the single phase of SBT for x=0.01and 0.03 and secondary phase of $Sr_3Ti_2O_7$ appeared when x>0.1. To compare the effect of Nb doping, the ferroelectric properties (hysteresis loop, piezoelectric coefficient) of Nb-doped SBT were measured. The SBT doped with x=0.15 was found to exhibit higher remanent polarization with d_{33}=17 pC/N.

Keywords Bismuth layer structure ferroelectrics (BLSF) · Dope · Ferroelectric properties

1 Introduction

$SrBi_4Ti_4O_{15}$(SBT) is one of Aurivillius family members, which is called the bismuth layer structure ferroelectrics (abbreviated as BLSF). The layered structure consists of $(Bi_2O_2)^{2+}$ layers interleaved with perovskite like ($A_{m-1}B_mO_{3m+1}$) layers, where A is a monovalent, divalent, or trivalent metallic ion, B is a tetravalent, pentavalent or hexavalent metallic ion that is located at the center of the oxygen octahedral, and m is the number of perovskite layers [1–3]. BLSF has potential use in device application because of their relative high Curie temperature, high dielectric breakdown strength, low dielectric loss, and high anisotropy. SBT, which contain four perovskite-like TiO_6 octahedron units stacked in between $(Bi_2O_2)^{2+}$ layers, has orthorhombic symmetry with space group A21am$\left(C_{2v}^{12}\right)a = 5.4280, b = 5.4380, c = 40.9400$Å [4] (Fig. 1).

PZT has a relatively low synthesis temperature of around 600 °C and shows a large remanent polarization (Pr), but it has the problem of fatigue with the Pt electrode to be overcome. SBT, on the other hand, shows excellent endurance on fatigue, but the relatively small Pr and high synthesis temperature hindered its commercial use. SBT have high creepage current and domain pinning resulting by defect. These defects, which were referenced as space charges, were captured at interface or grain boundary. Many investigations have indicated that oxygen vacancies act as space charge, which causes strong domain pinning. Theoretical calculation suggested that the increase in defect concentration leads to a decrease in 2 Pr. Substitution Ti^{4+} ion by high valence ion could counteract some defects that lead to fatigue and domain pinning.

In the present study, the structure and ferroelectric property of Nb-doped SBT were studied by XRD, XPS, Raman spectrum, piezoelectric coefficient and hysteresis loop.

2 Experimental

SBT and Nb-doped SBT ceramics were produced by conventional solid state method. Oxide mixture of Bi_2O_3, TiO_2, $SrCO_3$ and Nb_2O_5 with 99% purity was used as the raw materials. The mixture was ball milled with alcohol for 24 h, dried, then calcined at 800~1000 °C for 2 h. After

H. Hao (✉) · H. Liu · S. Ouyang
State Key Laboratory of Advanced Technology for Materials Synthesis and Processing, Material Science and Engineering School, Key Laboratory for Silicate Materials Science and Engineering, Wuhan University of Technology,
Wuhan 430070, People's Republic of China
e-mail: haohua@whut.edu.cn

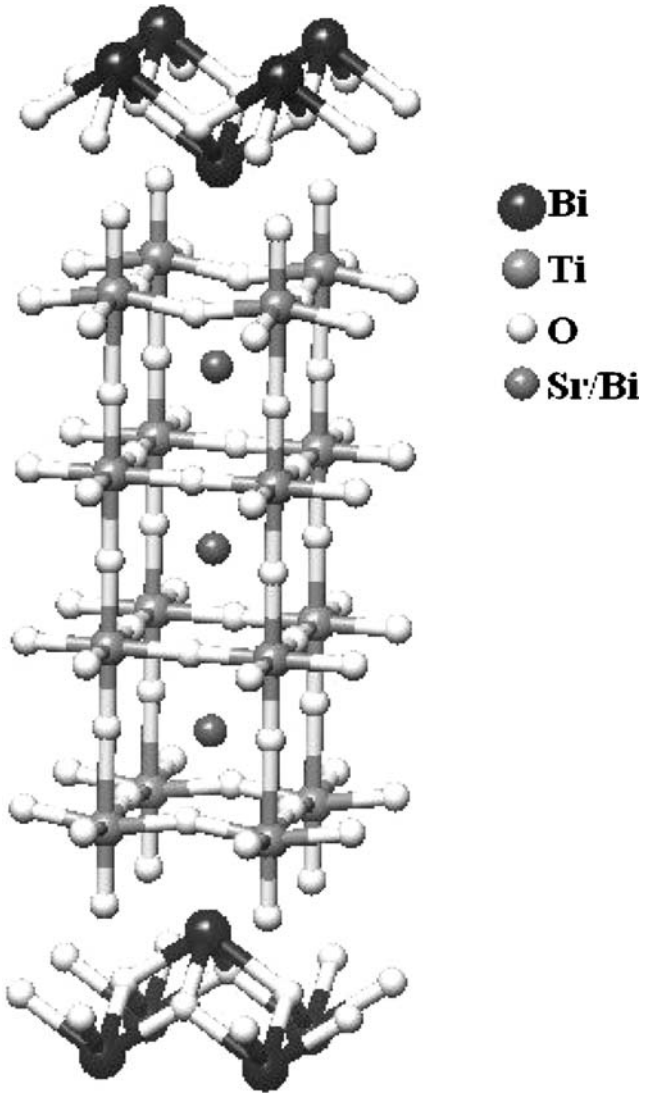

Fig. 1 Crystal structure of SBT

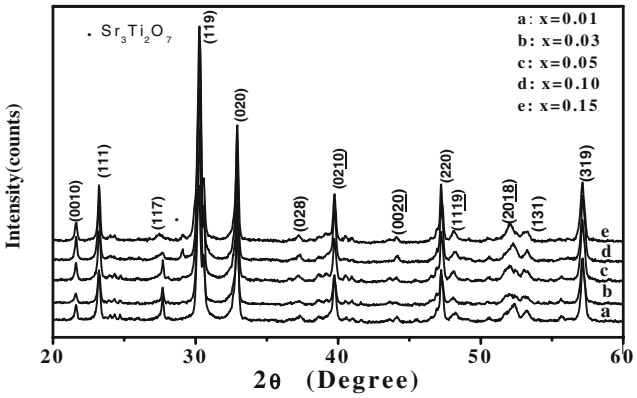

Fig. 3 XRD patterns of $SrBi_4Ti_{4-x}Nb_xO_{15}$

dried, the powders were pressed into pellets 15 mm in diameter and about 2 mm in thickness. These pellets were conventionally sintered at 1000~1200 °C temperature for 2~3 h. The density of the sintered pellet was measured via the Archimedes method, using distilled water and a balance with precision of $\pm 10^{-4}$. The relative density of the samples was the ratio of density to theory density (ρ=7.45 g/cm^3, obtained from X-ray measurements).

The sintered pellets were subjected to XRD analysis using Cu Kα radiation (PANalytical X'Pert PRO). Narrow region slow scanning XRD analysis was employed using Si as standard sample and testing condition was 0.01/step with 20 s. Piezoelectric properties of samples were poled on polished disks electroded with Ag paste by applying a direct-current (dc) electric field of 3~4 kV/mm for 30 min, in silicone oil, at 170 °C. The piezoelectric constant (d_{33}) was measured using a d_{33} meter Model ZJ-2. Hysteresis loop was measured by Radiant precision work station. Temperature dependence of the permittivity was tested by Agilent 4294A. The Raman measurements were performed using a RENISHAW Raman Microscope with testing condition excitation source 632.8 nm, He–Ne laser 17 mW, grating 1800 l/mm.

3 Results and discussion

The density of samples thus obtained was over 97% of the theoretical value. Surface morphology of Nb-doped SBT was detected by SEM (Fig. 2). It shows that the plate-like

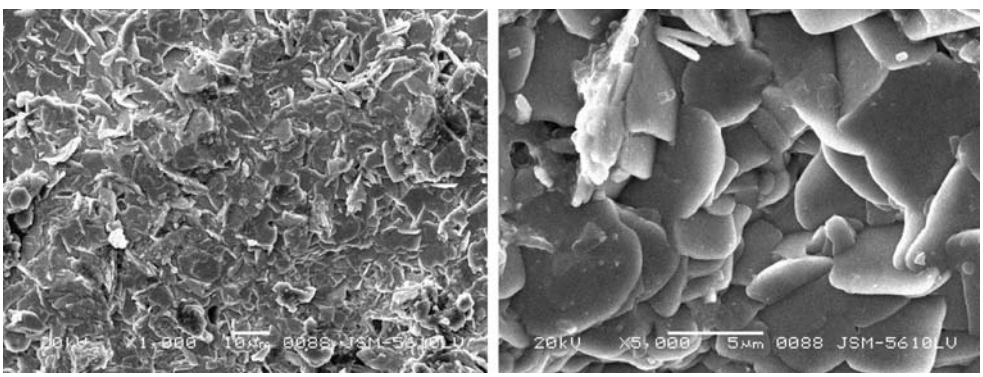

Fig. 2 SEM photographs of Nb-doped SBT ceramics

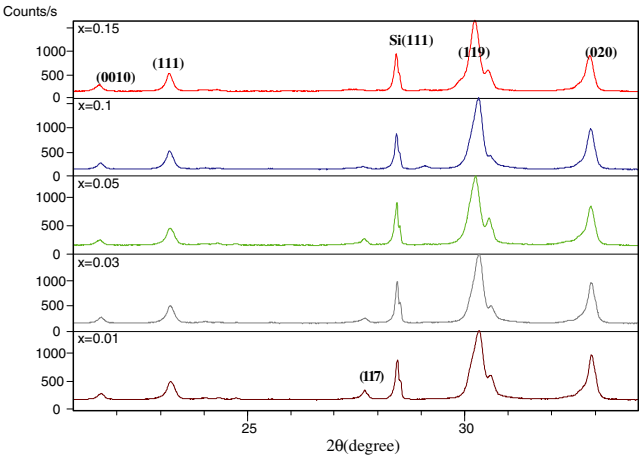

Fig. 4 Narrow slow scanning XRD of Nb-doped SBT

grain is distinct and defects of surface after sintering are hardly found.

3.1 Structure features of Nb-doped SBT

The tolerance factor, t, for the perovskite type structure is given by

$$t = (\bar{r}_A + r_O)\Big/\sqrt{2}(\bar{r}_B + r_O)\ 0.9 \le t \le 1.1$$

where $\overline{r_a}$;$\overline{r_b}$ and r_o are ionic radius of an average A-site cation, an average B-site cation, and an oxygen ion, respectively. For perovskite structure ABO_3, t changes from 0.9 to 1.10.However, for restriction of (Bi_2O_2) layer, the range of BLSF's t is narrowed in 0.81~0.93 [5]. In Nb-doped SBT, r_A is 0.096 nm (Bi^{3+}) or 0.113 nm (Sr^{2+}), r_B is 0.068 nm (Ti^{4+}) or 0.07 nm (Nb^{5+}) and r_0 is 0.14 nm. Obviously, the tolerance factor of SBT is 0.868.

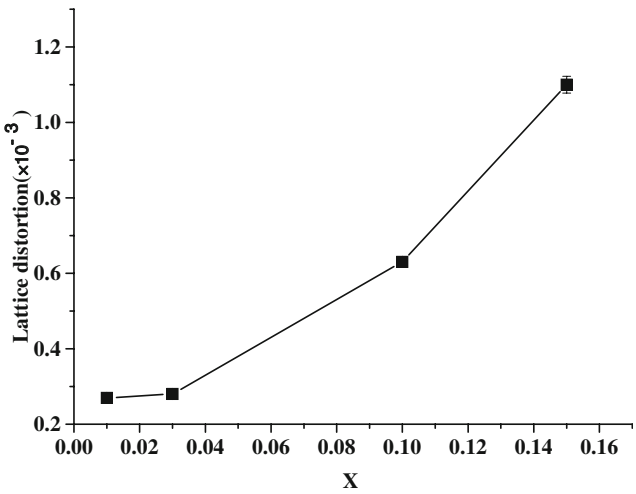

Fig. 5 Lattice distortion of Nb-doped SBT

Table 1 Lattice parameters of Nb-doped SBT.

	a(Å)	b(Å)	c(Å)
x=0.01	5.4449	5.4420	41.080
x=0.03	5.4446	5.4424	41.082
x=0.05	5.4448	5.4434	41.079
x=0.10	5.4482	5.4456	41.103
x=0.15	5.4509	5.4462	41.114

The XRD patterns of the samples show clear SBT phase (Fig. 3), indicating that Nb substitution do not change the structure of SBT or generate new phases. The results indicate the formation of the single phase of SBT for x= 0.01and 0.03; and secondary phase of $Sr_3Ti_2O_7$ appears when x>0.10. The coincidence of diffraction peaks for different x imply that Nb doping do not affect the basic crystal structure [6]. This is because that the Nb content is very low and the ions radius of Nb^{5+} and Ti^{4+} are closed to each other (Nb^{5+}: 0.070 nm, Ti^{4+}: 0.068 nm). Due to Nb^{5+} substituting Ti^{4+}could result emergency of titanium vacancy, there is affluent Ti when the substitution amount increases. Bismuth ion is easy to vapor at high temperature so affluent Ti would react into $Sr_3Ti_2O_7$.

We employed narrow region slow scanning XRD to calculate the lattice parameters of Nb-doped SBT. Choosing (111), (311) and (331) peaks of Si as standard to revise and according to XRD reference code 043-0973 of SBT, (0010), (020) and (319) peaks of SBT were applied to calculate the a, b, c using $\frac{1}{d^2} = \frac{h^2}{a^2} + \frac{k^2}{b^2} + \frac{l^2}{c^2}$. Because of larger ion radius of Nb^{5+} than Ti^{4+}, we can see from Fig. 4 that peaks shift slightly to lower degree. Compared with standard sample with a=5.4280 Å, b=5.4380 Å, c=40.9400 Å, a, b, and c of SBT with different substitution amount all increase, which is resulted by ion radius difference. a, b, and c change no obvious when $x \le 0.05$ and when x>0.10 the lattice parameters increase obviously which is consistent with Fig. 3. Hall method is employed to calculate the lattice distortion using $\frac{\beta\cos\theta}{\lambda} = \frac{K}{L} + \frac{4e\sin\theta}{\lambda}$, where L is grain size; e is lattice distortion; K=1; λ=1.5406 Å; β=B−b, B is the half high peak width of the sample, b is half high peak width of the Si standard sample. Figure 5 indicates that the lattice distortion increases with x grown and changes remark when x=0.15, which is coincident with the lattice parameter. All these prove that Nb doped SBT remains the SBT structure and lattice parameters, lattice distortion change a little when x<0.15 (Table 1).

Comparing with $SrBi_2Nb_2O_9$(SBN), It was shown by XPS spectrums of Nb element (Fig. 6) of doped-SBT that Nb^{5+} ion substituted Ti^{4+} ion and formed NbO_6 octahedron. In the spectrum, 209.65 and 206.93 eV peak is respectively corresponding to $3d_{3/2}$ and $3d_{5/2}$ electronic bonding energy. Peak position and ΔE_b of both spectrums are approximate.

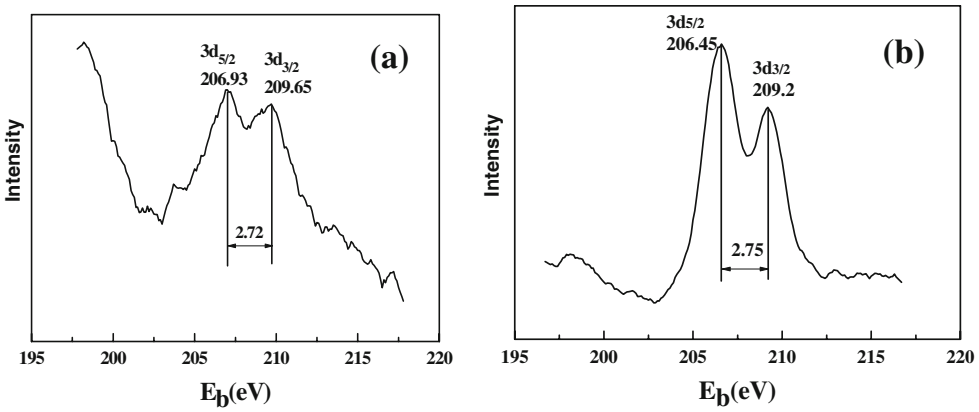

Fig. 6 XPS spectrums of Nb element (**a**) Nb-doped SBT; (**b**) SBN

The perovskite layer of SBN is composed of two NbO_6 octahedron layer and one NbO_6 octahedron neared the other NbO_6 octahedron and (Bi_2O_2) layer. Chemistry atmosphere is different from Nb-doped SBT and this results the higher Nb bonding energy of Nb-doped SBT.

The B-site composition dependence of the Raman spectra of $SrBi_4Ti_{4-x}Nb_xO_{15}$ (x=0.0, 0.01, 0.03, 0.05, 0.10, 0.15) was measured at room temperature (Fig. 7). Compared to SBT, the most prominent feature is the wider trend of all the modes with increasing Nb content. As for $SrBi_4Ti_4O_{15}$, E_g modes in the range 200–400 cm^{-1} have been assigned to O–Ti–O bending and the modes in the range 470–490 cm^{-1} were described as Ti–O torsional modes. The modes at 314 and 464 cm^{-1} can be attributed to the rotating and tilting of TiO_6 octahedral. The sharp peak at 870 cm^{-1} has A_{1g} character and represents the symmetric stretch of the TiO_6 octahedral [7]. After Nb-doping, the 270 cm^{-1} mode shifts opposite to lower wave number. The 870 cm^{-1} mode also becomes asymmetric with Nb substitution. As this mode originates from a symmetric stretching of BO_6 (B=Ti, Nb) octahedra, the higher wave number of this mode show the occupation of B-sites by lighter Nb ions. Not all of the BO_6 octahedra could be occupied by single ions in partially doped samples. Therefore, the presence of both the ions at B-sites results in two stretching wave numbers, leading to asymmetry [8–10].

All the testing results concerned with the structure indicate that Nb ions substitute into the Ti sites in TiO_6 octahedra and remain the structure of SBT.

3.2 Ferroelectric property of Nb-doped SBT

It is known that the piezoelectric properties of SBT are poor. One of the reasons is that the restriction of the permissible rotations of the spontaneous polarization in two dimensions (a–b plane) as compared to the freedom along all three dimensions in the ferroelectrics of the perovskite

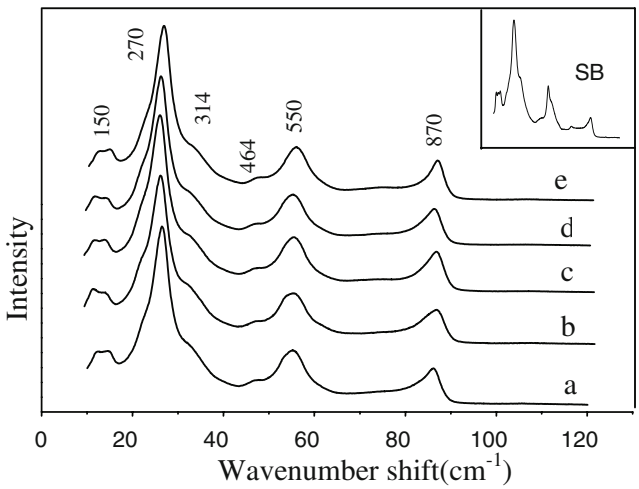

Fig. 7 Raman spectra of $SrBi_4Ti_{4-x}Nb_xO_{15}$ (*a*) x=0.01; (*b*) x=0.03; (*c*) x=0.05; (*d*) x=0.10; (*e*) x=0.15

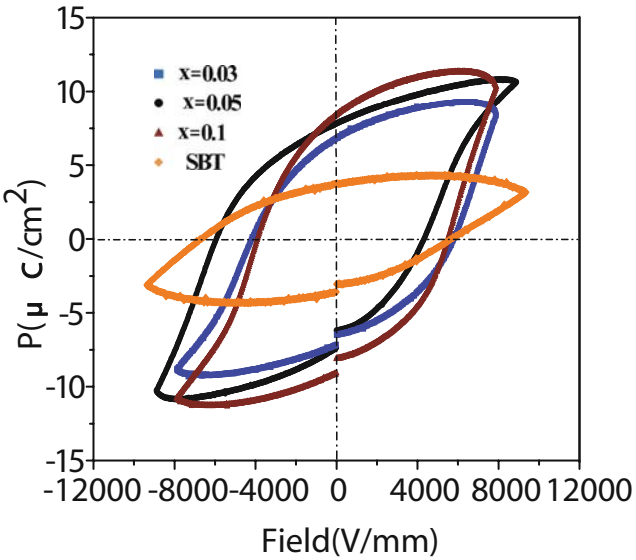

Fig. 8 Hysteresis curve of $SrBi_4Ti_{4-x}Nb_xO_{15}$

type compounds. Many investigations have indicated that oxygen vacancies act as space charge, which causes strong domain pinning. Theoretical calculation suggested that the increase in defect concentration leads to a decrease in 2 Pr [11, 12]. So the restraint of oxygen vacancies due to Nb doping bring about the increase in 2 Pr (Fig. 8). Spontaneous polarization of BLSF is mainly because O–Ti–O movement along *ab* plane. Titanium vacancy and bismuth vacancy resulted by Nb-doping would make *ab* plane ion transplant more easier and spontaneous polarization would increase. On the other hand, at high temperature bismuth oxide volatilization also lead to oxygen vacancy, which resulted domain pinning and restrained a part domain turning. Nb-doping could reduce the oxygen vacancy concentration and make domain turning more easy, residual polarization increased, but coercive field also increased after doping. This makes poling at higher electric field. Both aspect make the piezoelectric property increased slowly (Fig. 9. d_{33} changed from 6 to 17 pC/N).

Bismuth vacancy and oxygen vacancy were considered to be highest movability charge and had great influence on polarization fatigue and conductivity. Sintering at high temperature, bismuth ion was easy to vapor and form bismuth vacancy. Due to Nb^{5+} substituting Ti^{4+} could reduce concentration of oxygen and bismuth vacancy and depress domain pinning, Nb-doping was an efficient means to decrease conductivity. Donor doping could make bulk resistance increase and endure higher electric field and increase poling electric field. These make domain turning more completely when poling.

Figure 10 shows temperature dependence of the permittivity of $SrBi_4Ti_{4-x}Nb_xO_{15}$ at 1 kHz frequency. Compared with the Curie temperature of SBT (530 °C), sharp permittivity peak of Nb-doped SBT with x=0.03 appears

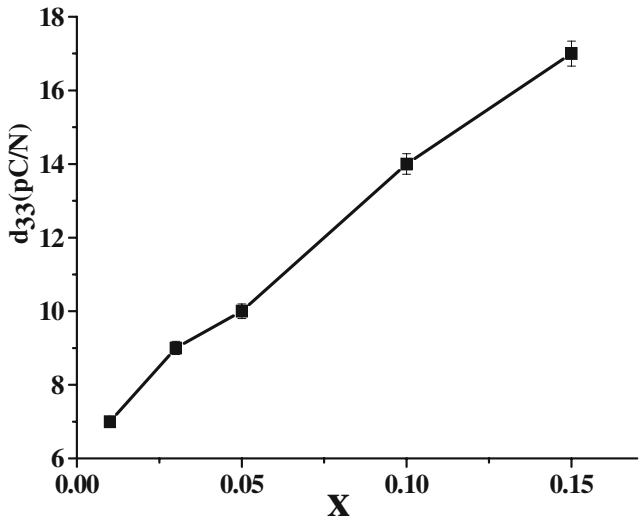

Fig. 9 Piezoelectric coefficient d_{33} of $SrBi_4Ti_{4-x}Nb_xO_{15}$

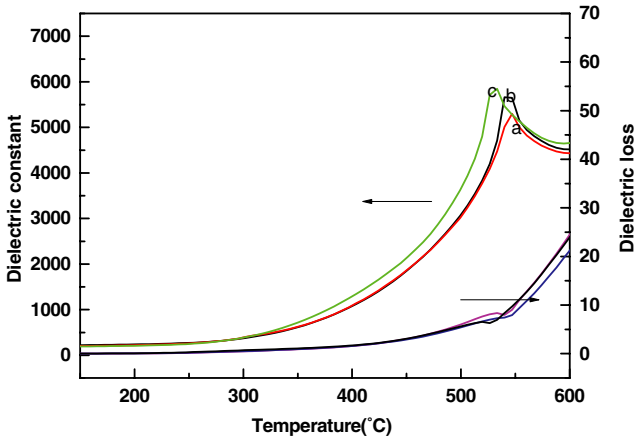

Fig. 10 Temperature dependence of the permittivity of $SrBi_4Ti_{4-x}Nb_xO_{15}$ (*a*) x=0.03; (*b*) x=0.05; (*c*) x=0.10

at about 520 °C and Tc decreases to about 500 °C when x increases. Because the Curie temperature is always found associated with the structure distortion, Nb-doping has little influence on the SBT structure. These is mainly because that ion radius of Nb^{5+} and Ti^{4+} is approximate and electronegative of both is approximatively the same (Nb 1.6, Ti 1.54).

4 Conclusion

Nb substitution do not change the structure of SBT or generate new phases. The XRD patterns indicates the formation of the single phase of SBT for x=0.01and 0.03; and secondary phase of $Sr_3Ti_2O_7$ appears when x>0.10. *a*, *b*, and *c* of SBT with different substitution amount all increases. It changes no obvious when $x \leq 0.05$ and when x>0.10 $Sr_3Ti_2O_7$ appears the lattice parameters increases obviously. Nb^{5+} ion substitutes Ti^{4+} ion and forms NbO_6 octahedron. Compared to SBT, the most prominent feature of the Raman spectra of $SrBi_4Ti_{4-x}Nb_xO_{15}$ is the wider trend of all the modes with increasing Nb content.

The restraint of oxygen vacancies due to Nb doping bring about the increase in 2 Pr. Nb-doping could reduce the oxygen vacancy concentration and make domain turning more easy, residual polarization increased, but coercive field also increases after doping. This makes poling at higher electric field. Both aspects make the piezoelectric property increased slowly. Having little influence on the SBT structure, Tc of Nb-doping decreases a little with x increased.

Acknowledgement The authors would like to acknowledge the support of the Natural Science Foundation of China (NSFC, Grant no. 50472016, 50502027), the main project of the Ministry of Education of China (MOE) and 973-Project (2002 CB613303) of China.

References

1. M.V. Gelfuso, J. Am. Ceram. Soc. **82**(9), 2368–2372 (1999)
2. T. Ogawa, J. Eur. Ceram. Soc. **24**, 1517–1520 (2004)
3. Ph. Boullay, G. Trolliard, D. Mercurio, J. Solid State Chem. **164**, 252–260 (2002)
4. C.H. Hervoches, A. Snedden, R. Riggs, S.H. Kilcoyne, P. Manuel, P. Lightfoot, J. Solid State Chem. **164**, 280–291 (2002)
5. A.S. Bhalla, R. Guo, R. Roy, Mat. Res. Innovat. **4**, 3–26 (2000)
6. Y.P. Chen, Y.Y. Yao, Z.H. Bao, P. Bao, J.S. Zhu, Y.N. Wang, Mater. Lett. **57**, 3623–3628 (2003)
7. H. Hao, H.X. Liu, M.H. Cao, X.M. Min, S.X. Ouyang, Appl. Phys. A **85**(1), 69–73 (2006)
8. P. S. Dobal, R. S. Katiyar, J. Raman Spectrosc. **33**, 405–423 (2002)
9. P.J. Klar, T. Rentschler, Solid State Commun. **103**(6), 341–345 (1997)
10. Y.L. Dua, G. Chena, M.S. Zhang, Solid State Commun. **131**, 313–317 (2004)
11. J. Zhu, X.-Y. Mao, X.-B. Chen, Solid State Commun. **130**, 363–366 (2004)
12. R.Z. Hou, X.M. Chen, Solid State Commun. **130**, 469–472 (2004)